

nuclei should be minimal in this case. The shake-off of the vacuum polarization cloud, which is a collective type of  $e^+e^-$  creation, is a new process of quantum electrodynamics. It is—so to speak—the real setting-free of vacuum polarization charges due to the Fourier frequencies in the collision.

We acknowledge fruitful discussions with Professor J. Greenberg (Gesellschaft für Schwerionenforschung) on the experimental observability of positron production in heavy-ion collisions and are grateful to Professor Werner Scheid, Gießen, for critical reading of the manuscript.

\*Supported by the Bundesministerium für Forschung und Technologie and by the Gesellschaft für Schwerionenforschung.

<sup>1</sup>B. Müller, H. Peitz, J. Rafelski, and W. Greiner, Phys. Rev. Lett. **28**, 1235 (1972).

<sup>2</sup>J. Rafelski, B. Müller, and W. Greiner, Nucl. Phys. **B68**, 585 (1974).

<sup>3</sup>Ya. B. Zel'dovich and V. S. Popov, Usp. Fiz. Nauk **105**, 403 (1971) [Sov. Phys. Usp. **14**, 673 (1972)].

<sup>4</sup>K. Smith, B. Müller, and W. Greiner, J. Phys. B **8**, 75 (1975).

<sup>5</sup>B. Müller, J. Rafelski, and W. Greiner, Phys. Lett. **B47**, 5 (1973); B. Müller and W. Greiner, Z. Naturforsch. **31a**, 1 (1976).

<sup>6</sup>W. Betz, G. Soff, B. Müller, and W. Greiner, Phys. Rev. Lett. **37**, 1046 (1976).

<sup>7</sup>The vector potential arising from the nonadiabaticity of the quasimolecule has been neglected. The transverse current  $\vec{j} - (4\pi)^{-1}\nabla\phi$  is by a factor  $v/c \sim 0.1$  smaller than the charge density  $\rho$ , i.e., the effective magnetic coupling constant is only  $Z\alpha v/c$  as compared to the electric  $Z\alpha$ .

<sup>8</sup>P. G. Reinhard, W. Greiner, and H. Arenhövel, Nucl. Phys. **A166**, 173 (1971).

<sup>9</sup>J. Bang and J. M. Hansteen, K. Dan. Vidensk. Selsk., Mat.-Fys. Medd. **31**, No. 13 (1959).

<sup>10</sup>V. M. Budnev, I. F. Ginzburg, G. V. Meledin, and V. G. Serbo, Phys. Rep. **15C**, 181 (1975).

<sup>11</sup>D. R. Bates and R. McCarroll, Proc. Roy. Soc. London, Ser. A **245**, 175 (1958).

<sup>12</sup>M. Gyulassy, Phys. Rev. Lett. **33**, 921 (1974); G. A. Rinker and L. Wilets, Phys. Rev. A **12**, 748 (1975).

## Positronium Spin Conversion by Phosphorescent Impurities in Gases\*

Werner Brandt and Dalia Spektor

*Department of Physics, New York University, New York, New York 10003*

(Received 22 October 1976)

Ultraviolet illumination of Ar, N<sub>2</sub>, or air containing trace amounts of SO<sub>2</sub> or benzaldehyde quenches positronium through interactions with photoexcited impurity triplet states. The measured interaction cross sections are large,  $\sim 10^4\pi a_0^2$ , and appear to increase as  $T^{1/2}$  in the range 300 to 400°K. Triplet concentrations as low as  $10^{-8}$  can be detected at atmospheric pressures.

We report first measurements of photomagnetic positronium quenching in argon, nitrogen, and air at atmospheric pressures containing small concentrations of benzaldehyde or SO<sub>2</sub>, which have metastable triplet states. The large cross sections are similar to those observed in solids<sup>1</sup> and pose intriguing new questions with regard to the quantum theory of excited molecular spin-state interactions with leptonic atoms. This work may have implications for research on gas pollution and, in particular, on H<sub>2</sub>SO<sub>4</sub> formation via the photodynamic oxidation of SO<sub>2</sub> to SO<sub>3</sub> in air.<sup>2</sup>

Suppose a gas contains a small concentration,  $c$ , of molecules or atoms in electronic singlet ground states ( $S=0$ ) that can be excited by light to populate metastable paramagnetic triplet states  $T^*$  ( $S=1$ ) at a steady-state concentration  $c_T \ll c$ . When  $o$ -Ps (orthopositronium; spin quantum number  $S=1$ ) interacts with  $T^*$ , it can be quenched

by spin conversion into  $p$ -Ps (parapositronium;  $S=0$ ) with efficiency  $\alpha_o$ , and  $p$ -Ps quenched into  $o$ -Ps with efficiency  $\alpha_p$ , by spin flip correlated with the quenching of  $T^*$ ,<sup>1</sup> or possibly by chemical binding of  $o$ -Ps to the excited molecule. In solids, the  $o$ -Ps lifetime is only 2 times longer than that of positrons in other states (1 nsec versus 0.5 nsec). In gases, it is  $\sim 100$  times longer (100 nsec versus 1 nsec). Therefore the "positronium method" ought to be more sensitive for the detection of photomagnetic impurities through  $o$ -Ps quenching in gases than in solids. The results reported here bear this out.

The experiments were performed as follows. A cylindrical copper chamber with length  $L$  of 25 cm and diameter of 10 cm was closed at one end by a copper plate which held the positron source, consisting of 5  $\mu$ Ci <sup>22</sup>Na deposited on an Al backing. The other end consisted of a quartz window

to admit the uv light from a high-pressure mercury lamp. Color and gray filters could be inserted between the lamp and the quartz window. The chamber was connected to a pumping and gas-mixing station to permit emptying, flushing, and filling with a carrier gas containing known amounts of "impurities." The chamber was charged at 295°K with 760 Torr of Ar, N<sub>2</sub>, or air; fillings with 380 and 1520 Torr of Ar were also studied. The admixtures were SO<sub>2</sub> or benzaldehyde, C<sub>6</sub>H<sub>5</sub>-CHO, henceforth abbreviated as  $\Phi$ CHO. An electric heating mantle enwrapped the chamber and kept the gas temperature constant at variable levels between 300 and 400°K through a feedback loop with a thermocouple in the chamber. One of two NaI(Tl) scintillators mounted on RCA 4524 photomultipliers was placed behind the <sup>22</sup>Na source, and the other next to the wall of the chamber. They recorded through a standard coincidence apparatus the time spectra of the delayed coincidences between the 1.28-MeV  $\gamma$  ray from the <sup>22</sup>Na source accompanying the emission of a positron, and one of the 0.511-MeV  $\gamma$  rays from the  $\gamma$  annihilations with electrons. The coincidences for times larger than a preset time delay,  $t_c$ , typically 30 nsec, were summed and stored. The experiment was repeated at intervals of several minutes with the light alternately on and off, until the total number of counts in each mode approached 10<sup>4</sup>. This choice of  $t_c$  eliminated positron annihilations from states other than *o*-Ps. The quenching results were independent of  $t_c$  in the range of 20 to 100 nsec. The extinction coefficient,  $\epsilon'$ , for the light in the absorption range of the impurities was such that  $\epsilon' L \ll 1$ , i.e., the density of photomagnetic impurities could be taken as constant throughout the gas. In the absence of these impurities, no photoinduced *o*-Ps quenching was observed.

The relative number of annihilations that occur at delay times  $t \geq t_c$  is given by

$$N(t_c) = I_1 \exp(-\Gamma_1 t_c) + I_2 \exp(-\Gamma_2 t_c) \approx I_2 \exp(-\Gamma_2 t_c), \quad (1)$$

where the short-lived component of intensity  $I_1$  subsumes all positron annihilations other than from *o*-Ps, with a mean disappearance rate  $\Gamma_1$ . The experiment is designed such that  $\Gamma_1 t_c \gg 1$ . The component of intensity  $I_2 = 1 - I_1$  encompasses the disappearance of *o*-Ps with rate  $\Gamma_2 \approx \gamma_o + \kappa_o$ , where  $\gamma_o$  is the *o*-Ps annihilation rate in the gas, and  $\kappa_o$  the *o*-Ps spin conversion rate.

The counts in the dark,  $N^{\text{off}}(t_c)$ , stem from *o*-

Ps annihilations via electron pickoff into two  $\gamma$  rays, each of energy 0.511 MeV at rate  $\gamma_{p,o}$  and by self-annihilation into three  $\gamma$  rays with a continuous energy distribution peaking at the cutoff 0.511 MeV, at rate  $\gamma_3 = (140 \text{ nsec})^{-1}$  so that  $\Gamma_2^{\text{off}} = \gamma_o = \gamma_{p,o} + \gamma_3$ . The counts under illumination,  $N^{\text{on}}(t_c)$ , reflect the increased two- $\gamma$  annihilation rate  $\Gamma_2^{\text{on}} = \gamma_o + \kappa_o$  due to *o*-Ps interactions with  $T^*$ . If  $\eta$  denotes the ratio of counts in the 0.511-MeV detector from two- $\gamma$  decays and from three- $\gamma$  decays, the count rates are related to  $\kappa_o$  as

$$\frac{N^{\text{on}}(t_c)}{N^{\text{off}}(t_c)} = \left( 1 + \frac{\kappa_o \eta}{\gamma_3 + \gamma_{p,o} \eta} \right) \frac{\Gamma_2^{\text{off}}}{\Gamma_2^{\text{on}}} \exp(-\kappa_o t_c). \quad (2)$$

In our experiments where  $\eta \approx 1$ , the forefactor in Eq. (2) was close to unity and insensitive to changes in  $\eta$  and  $\kappa_o$ . This was confirmed by shifting the detector energy-acceptance window. Therefore, we extract from the data the photoinduced *o*-Ps quenching rate according to

$$\kappa_o = \Gamma_2^{\text{on}} - \Gamma_2^{\text{off}} = \frac{1}{t_c} \ln \frac{N^{\text{off}}(t_c)}{N^{\text{on}}(t_c)}. \quad (3)$$

Experimental and theoretical elastic Ps-Ar scattering cross sections<sup>3</sup> suggest that spin conversion in our systems is not Ps-diffusion-limited, but dominated by direct processes with quenching rate<sup>4</sup>

$$\kappa_o = \nu_T n_T = n_T v_{Ps} \alpha_o \sigma_T, \quad (4)$$

in terms of the volume rate  $\nu_T$  and cross section  $\sigma_T$  for Ps spin conversion by  $T^*$  present at density  $n_T$ ,  $v_{Ps}$  being the Ps group velocity;  $\alpha_o \sigma_T$  is the respective *o*-Ps quenching cross section. Indeed, the experiments prove that Eq. (3) is independent of the carrier gas. Its function is to slow down positrons to form significant amounts of Ps in the chamber. In the presence of a density  $n_P$  of phosphor molecules, the  $T^*$  density is given by

$$n_T = \varphi_T \tau_T A n_P, \quad (5)$$

where  $\varphi_T$  is the triplet yield,  $\tau_T$  is the phosphorescence lifetime, and  $A$  is the absorbed light intensity

$$A = \int g(\omega) \epsilon(\omega) d\omega \quad (6)$$

from a lamp emitting photons with spectral intensity distribution  $g(\omega)$ , by phosphor molecules with photoabsorption cross section  $\epsilon(\omega)$  at frequency  $\omega$ .

Figure 1 demonstrates that the change  $(N^{\text{on}} - N^{\text{off}})/N^{\text{off}} \approx -\kappa_o t_c$  in Ar increases linearly with

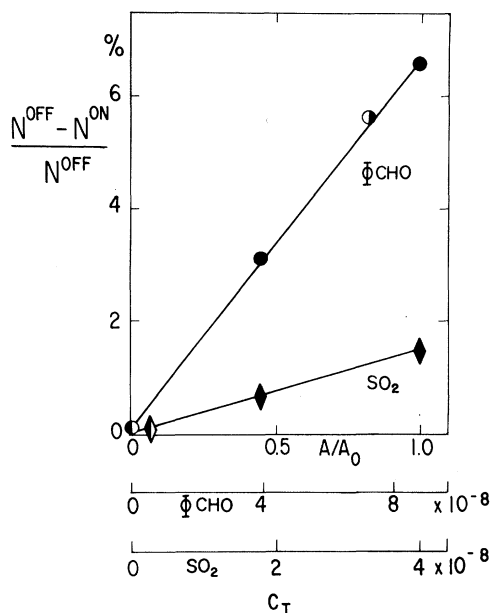


FIG. 1. Light-induced relative changes of counting rates, to first order equal to  $\kappa_o t_c$  with  $t_c = 30$  nsec, as a function of the relative light absorption  $A/A_0$ , Eq. (6). The maximum absorption  $A_0 = 4 \times 10^{-2}$  photons/sec per benzaldehyde,  $\Phi\text{CHO}$ , and  $A_0 = 7 \times 10^{-3}$  photons/sec per  $\text{SO}_2$  inside the chamber is known to  $\pm 25\%$ . Data given as solid symbols pertain to the full lamp spectrum with and without gray filters, right-hand half-open symbols to filters (Corning CS 3-74 for  $\Phi\text{CHO}$  and CS 0-54 for  $\text{SO}_2$ ) transmitting the light at lower frequency than the phosphor absorption edge, and the left-hand half-open symbol to a filter (Corning CS 7-54) transmitting at higher frequencies. The lower scales are nomograms for the relations between  $A$  and  $c_T$  in Ar at 1 atm and  $T = 300^\circ\text{K}$ . Relative errors are comparable to the size of the symbols.

the absorption. We changed  $A$  relative to its maximum value  $A_0$  by reducing the light intensity with gray filters (full symbols), or by changing the spectral distribution through interference filters with transmission at frequencies lower than the impurity absorption edge (right-hand open symbols) or higher than the absorption edge (left-hand open symbol). The effect is specific. It is linked to the action spectrum of the system in that only light absorbed by the phosphor leads to  $o$ -Ps quenching. The method can detect changes of a few  $T^*$  molecules in  $10^8$  gas molecules. Variations in the light intensity at the Ps Lyman absorption line had no measurable effect on  $\kappa_o$ .

Figure 2 displays the experimental volume rates  $\nu_T = \kappa_o/n_T$ , where  $\kappa_o$  is given by the right-hand side of Eq. (3), and  $n_T$  is calculated from Eq. (5) with the phosphor parameters  $\tau_T$ ,  $\varphi_T$ ,

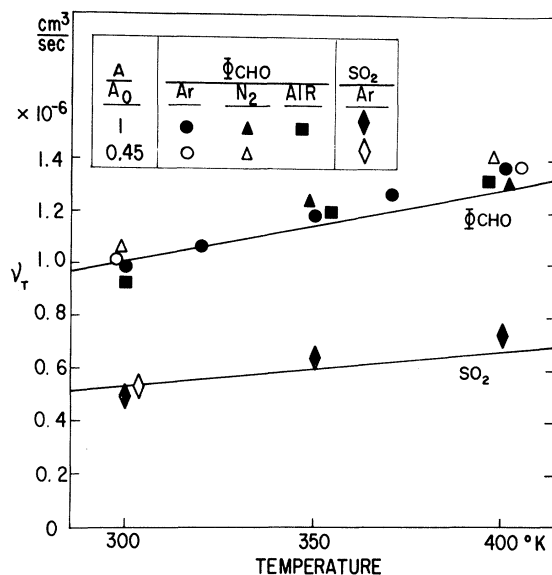


FIG. 2. Volume rates  $\nu_T = \kappa_o/n_T$  for spin conversion of  $o$ -Ps by benzaldehyde ( $\Phi\text{CHO}$ ) and  $\text{SO}_2$  in photoexcited triplet states as a function of temperature in Ar,  $\text{N}_2$ , and air at 48% relative humidity, with constant density equal to that at 760 Torr and  $295^\circ\text{K}$ . The scatter of the points at a given temperature is indicative of their relative uncertainties. The absolute values carry the uncertainties of  $A_0$  through  $n_T$ , which can be inferred from the nomograms in Fig. 1. The solid lines are calculated from Eq. (8) with interaction radii  $R_T = 40^\circ$  for  $\Phi\text{CHO}^*$  and  $R_T = 30 \text{ \AA}$  for  $\text{SO}_2$ .

and  $\epsilon(\omega)$  taken from literature,<sup>5</sup> and  $g(\omega)$  calibrated as in the earlier work.<sup>1</sup> Evidently,  $\nu_T$  is independent of the carrier gas and the partial pressure of the impurity; it rises with temperature,  $T$ , approximately as  $T^{+1}$ . Table I summarizes the range of our experimental conditions. It lists the mean values of  $\nu_T$ . The resulting Ps- $T^*$  quenching cross sections are  $\sim 10^{-12} \text{ cm}^2 = 10^4 \pi a_0^2$ , where  $a_0$  is the Bohr radius. They signify interaction ranges of  $50 \text{ \AA}$ . Table II compares known  $o$ -Ps quenching efficiencies and cross sections of gas molecules<sup>6</sup> by electron pickoff [ $\text{N}_2$  ( $S=0$ ); Ar ( $S=0$ )] and by ground-state spin conversion [ $\text{O}_2$  ( $S=1$ ); NO ( $S=\frac{1}{2}$ )] with our results for the quenching by excited triplets [ $\Phi\text{CHO}^*$  ( $S=1$ );  $\text{SO}_2^*$  ( $S=1$ )].

To gain perspective on the trends in Fig. 2, we adapt the cross section given earlier<sup>4</sup> for an extended center of effective size  $2R_T$  exerting a short-range attraction on neutral Ps, of de Broglie wavelength  $k_{\text{Ps}}^{-1} = \hbar/m_{\text{Ps}} v_{\text{Ps}}$  with  $m_{\text{Ps}} = 2m_e$ . The attraction expressed as a Ps- $T^*$  affinity  $\Delta$  is related to the Ps wave vector,  $K$ , in close  $T^*$  proximity as  $\Delta = (\hbar K)^2/2m_{\text{Ps}}$ . In this stylized model,

TABLE I. Summary of experimental conditions.

Phosphor	$\varphi_T^a$	$\tau_T^a$ ( $10^{-3}$ sec)	Carrier gas <sup>b</sup>	Parameters varied <sup>c</sup>	$c_T$ (ppm)	$\nu_T^d$ ( $10^{-6}$ cm <sup>3</sup> /sec)	$\sigma_T^d$ ( $10^{-12}$ cm <sup>2</sup> )
$\Phi$ CHO	0.95	2.1	Ar	$T, A, n_G, t_c$	0.05–20	$1.2 \pm 0.3$	$1.5 \pm 0.4$
			N <sub>2</sub>	$T, A$	0.05–0.1		
			Air <sup>e</sup>	$T$	0.1		
SO <sub>2</sub>	0.015	1.7	Ar	$T, A$	0.02–0.04	$0.6 \pm 0.2$	$0.9 \pm 0.3$

<sup>a</sup>Calculated from optical rate constants given in Ref. 5.

<sup>b</sup>At constant density  $n_G = 2.45 \times 10^{19}$  molecules/cm<sup>3</sup> corresponding to 760 Torr at 295°K. Measurements at  $\frac{1}{2}n_G$  and  $2n_G$  in Ar showed no change in  $\nu_T$ .

<sup>c</sup>Quenching depends only on the density of triplets  $n_T$ , related to the phosphor density  $n_p = cn_G$  as given by Eq. (5) and to  $c_T$  as  $n_T = c_T n_G$ .

<sup>d</sup>Mean value in the range 300 to 400°K (cf. Fig. 2). In Ar,  $\nu_T$  remained independent of the gas pressure between 380 and 1520 Torr, i.e.,  $\tau_T$  can be taken to be a constant under our conditions.

<sup>e</sup>At 48% relative humidity.

the volume rate becomes

$$\nu_T = \alpha_o v_{Ps} \sigma_T = \alpha_o \frac{4\pi\hbar}{m_{Ps}K} \left( \frac{1 + R_T k_{Ps}}{1 + K^{-1} k_{Ps}} \right)^2 \quad (7)$$

With  $v_{Ps} = (3k_B T/m_{Ps})^{1/2}$ ,  $\Delta \sim 0.3$  eV and  $\alpha_o = 0.1$ ,<sup>1</sup> Eq. (7) takes the form

$$\nu_T = a \left( \frac{1 + bR_T \sqrt{T}}{1 + c\sqrt{T}} \right)^2 \quad (8)$$

(where  $T$  is given in degrees Kelvin) in terms of the constant  $a = 1.8 \times 10^{-8}$  cm<sup>3</sup>/sec,  $b = 8.2 \times 10^5$  cm<sup>-1</sup> deg<sup>-1/2</sup>, and  $c = 2 \times 10^{-2}$  deg<sup>-1/2</sup>. Equation (8) yields the solid lines in Fig. 2 with  $R_T = 40$  Å for  $\Phi$ CHO\* and  $R_T = 30$  Å for SO<sub>2</sub>\*.

In summary, the interaction of Ps with photoexcited triplet states of molecules leads to Ps quenching. One may attribute this effect to spin flip, an exothermic process in which a phosphorescent triplet state is converted concomitantly into the singlet ground state. The quenching rates of *o*-Ps can be measured selectively in gases with high sensitivity because of the long *o*-Ps lifetimes. Compared to Ps spin-conversion

cross sections of molecules in triplet ground states, such as O<sub>2</sub>, the cross sections we observe here are large and permit detection of photomagnetic trace impurities even in air. Their magnitude and  $T^{1/2}$  dependence appear to be linked to the fact that Ps is a neutral quantum mechanical probe. One concludes that photoinduced Ps quenching is a new general phenomenon that occurs in gases and solids. The detailed analysis must await fresh theoretical developments and measurements of continuous-action spectra on possibly simpler systems than those chosen to uncover the effect.

We are grateful to A. Schwarzschild for discussions.

\*Work supported by the National Science Foundation.

<sup>1</sup>W. Brandt and P. Kliauga, Phys. Rev. Lett. **30**, 354 (1973), and Phys. Rev. B **14**, 884 (1976).

<sup>2</sup>H. W. Sidebottom, C. C. Badcock, G. G. Jackson, J. G. Calvert, G. W. Reinhart, and E. K. Damon, Environ. Sci. Technol. **6**, 72 (1972).

TABLE II. Comparison of *o*-Ps quenching rates and cross sections of ground-state molecules (Ref. 6) with those of molecules in photoexcited triplet states (\*) at 300°K.

Molecule	S	<i>o</i> -Ps quenching rate ( $10^6$ atm <sup>-1</sup> sec <sup>-1</sup> )	Quenching cross section ( $10^{-21}$ cm <sup>2</sup> )
N <sub>2</sub>	0	$2.1 \times 10^{-1}$	1.1
Ar	0	$2.5 \times 10^{-1}$	1.4
O <sub>2</sub>	1	$1.8 \times 10^1$	$1.0 \times 10^2$
NO	$\frac{1}{2}$	$2.5 \times 10^3$	$1.4 \times 10^4$
SO <sub>2</sub> *	1	$1.1 \times 10^7$	$6.0 \times 10^7$
$\Phi$ CHO*	1	$1.8 \times 10^7$	$9.7 \times 10^7$

<sup>3</sup>D. M. Spektor and D. A. L. Paul, *Can. J. Phys.* **53**, 13 (1975).

<sup>4</sup>W. Brandt, *Appl. Phys.* **5**, 1 (1974).

<sup>5</sup>M. Stockburger, *Z. Phys. Chem.* **31**, 350 (1962) (CO); T. N. Rao, S. S. Collier, and J. G. Calvert, *J. Am. Chem. Soc.* **91**, 1616 (1969) (SO<sub>2</sub>); *Absorption Spectra in the Ultraviolet and Visible Region*, edited

by L. Lang (Academic, New York, 1961). We thank N. Geacintov and W. Losonsky for discussions on the properties of triplet SO<sub>2</sub>\* and ΦCHO\*.

<sup>6</sup>G. J. Celians and J. H. Green, *Proc. Phys. Soc., London* **83**, 823 (1964) (N<sub>2</sub>, Ar); F. F. Heymann, P. E. Osmon, J. J. Veit, and W. F. Williams, *Proc. Phys. Soc., London* **78**, 1038 (1961) (O<sub>2</sub>, NO).

## Hydrodynamic Instabilities in Coulomb Fluids

B. A. Huberman and W. Streifer

*Xerox Palo Alto Research Center, Palo Alto, California 94304*

(Received 16 December 1976)

We show that a poorly electrically conducting fluid, in the presence of both static thermal and potential gradients, displays instabilities that are very different from those encountered in the Rayleigh-Bénard problem. For certain parameter values, we predict a direct transition to oscillatory behavior which should be observable by simple means.

A set of interesting flow patterns unfolds as a viscous fluid undergoes the transition from the laminar to the turbulent state. Although the threshold sequence of instabilities is not universal, the Rayleigh-Bénard problem provides a good illustration. In this case a fluid layer in the presence of a thermal gradient undergoes a transition to time-independent convective flow under sufficiently large thermal stresses as measured by the Rayleigh number. With increasing values of this parameter the flow becomes oscillatory in character and then eventually attains a fully turbulent state. Recently some of these instabilities have been analyzed in detail both theoretically and experimentally in fluids that span a large spectrum of Prandtl numbers.<sup>1-6</sup>

The above scheme is greatly modified when one considers a fluid containing mobile charges in the presence of an externally applied potential. In particular, the case of low-mobility systems, such as weak ionic solutions or electrophoretic cells,<sup>7</sup> provides a new set of interesting phenomena. In such Coulomb fluids<sup>8</sup> the persistence of charge-density fluctuations and their associated fields for times that are comparable to those of fluid motion leads to additional dissipative processes and restoring forces which change the nature of the instabilities.

In this Letter we analyze the stability of a Coulomb fluid in the presence of both thermal and electric potential gradients. As we show, the new degree of freedom provided by the charges leads not only to renormalized convective thresholds but also to a novel type of instability. Specifically, for certain parameter values an oscillatory

regime develops in which the Coulomb forces acting on the double layer of the fluid subtly compensate the buoyancy term. Besides their intrinsic interest, the fact that the oscillations can be easily detected by electrical means provides a new experimental tool for studying flow instabilities.

We consider a typical Bénard geometry with free boundaries of infinite lateral extent and separated by a distance  $h$  along the vertical  $z^*$  axis, and which are good conductors of both electric charges and heat. The cell is filled with a fluid of dielectric constant  $\epsilon$ , viscosity  $\nu$ , and thermal diffusivity  $\kappa$ . The fluid density is  $\rho_0^*$  and it contains a number density  $n_0^*$  of equal positive and negative charges of magnitude  $Ze$ . The mobility of the charged carriers is in turn given by  $\mu = (Ze)^2 D / k_B T_0$  with  $D$  their diffusion coefficient in the fluid and  $T_0$  its mean temperature. Besides the customary temperature difference  $\Delta T$  there exists an electric field  $E$  throughout the fluid which is produced by an applied potential difference  $V_0$  between the two plates. We further assume the fluid-plate interface to be nonohmic.

In the absence of any convective currents and for the geometry outlined above, the potential through the fluid is given within the Debye-Hückel approximation by

$$\varphi_s^*(z^*) = \frac{V_0}{2} \frac{\sinh[\sqrt{2}(z^* - h/2)/\xi]}{\sinh[\sqrt{2}h/2\xi]}, \quad (1)$$

with  $0 \leq z^* \leq h$  and  $\xi$  the screening length, which is given by  $\xi^{-2} \equiv n_s^*(Ze)^2 / \epsilon k_B T_0$ . Similarly the static charge density  $n_s^*(z^*)$  is given through Poisson's equation by  $n_s^*(z^*) = -2(Ze)^2 n_0^* \varphi_s^*(z^*)$